ADVANCED FUNCTIONAL MATERIALS
www.afm-journal.de

Self-Healing Materials via Reversible Crosslinking of Poly(ethylene oxide)-*Block*-Poly(furfuryl glycidyl ether) (PEO-*b*-PFGE) Block Copolymer Films

*Markus J. Barthel, Tobias Rudolph, Anke Teichler, Renzo M. Paulus, Jürgen Vitz, Stephanie Hoeppener, Martin D. Hager, Felix H. Schacher * and Ulrich S. Schubert**

The application of well-defined poly(furfuryl glycidyl ether) (PFGE) homopolymers and poly(ethylene oxide)-*b*-poly(furfuryl glycidyl ether) (PEO-*b*-PFGE) block copolymers synthesized by living anionic polymerization as self-healing materials is demonstrated. This is achieved by thermo-reversible network formation via (retro) Diels-Alder chemistry between the furan groups in the side-chain of the PFGE segments and a bifunctional maleimide crosslinker within drop-cast polymer films. The process is studied in detail by differential scanning calorimetry (DSC), depth-sensing indentation, and profilometry. It is shown that such materials are capable of healing complex scratch patterns, also multiple times. Furthermore, microphase separation within PEO-*b*-PFGE block copolymer films is indicated by small angle X-ray scattering (lamellar morphology with a domain spacing of approximately 19 nm), differential scanning calorimetry, and contact angle measurements.

1. Introduction

The capability to heal inflicted damage is ubiquitous in nature as, e.g., shown via the merging of broken bones, the closure of injured blood vessels,[1–3] or the healing of byssal threads of marine mussels.[4] The present awareness that the availability of raw materials will decrease, accompanied by increasing material and production costs, renders self-healing approaches an attractive research field in polymer chemistry and materials science. Particular interest is devoted to the facile introduction of such features into mechanically robust polymeric systems whilst maintaining synthetic feasibility and, even more important, processability of the resulting materials.

Different methods have been reported to introduce self-healing properties to a polymeric material.[5–7] One possibility is the encapsulation of reactive ingredients (a polymerizable healing agent and an initiator) within the desired material. Scratching or crack formation leads to a release of the embedded substances (e.g., by rupture of microcapsules), followed by mixing of both ingredients and resulting in a healing process of the damaged material.[8] This approach was also extended by the introduction of vascular networks containing a healing agent, which was released upon rupture.[9] Therefore, multiple healing processes are possible. A second approach represents the use of intermolecular forces. For this purpose, reversible interactions (i.e., crosslinks) of polymer chains with, e.g., hydrogen bonds represent a widely used strategy. After being damaged, these bonds allow a healing due to the reformation of bonds without any external stimuli such as heating or irradiation being necessary. This has been achieved using highly specific donor-acceptor systems,[10–15] and could recently be also applied for "hard" epoxy networks.[16] Another example of this approach are metal-ligand interactions. Thereby, materials consisting of polymers or oligomers comprising reversible non-covalent metal-ligand interactions (e.g., 2,6-bis(1′-methylbenzimidazolyl)pyridine or terpyridine, as well as corresponding metal ions) can heal inflicted damage.[17,18] Also, this ability represents an inherent material characteristic (i.e. intrinsic self-healing materials) and does not require the encapsulation of external healing agents. Moreover, the application of π–π interactions in self-healing processes has also been demonstrated for, e.g., pyrenyl units which interact with naphthalene diimide oligomers to reversibly crosslinked polymeric networks.[19,20]

M. J. Barthel, T. Rudolph, A. Teichler, R. M. Paulus, Dr. J. Vitz, Dr. S. Hoeppener, Dr. M. D. Hager, Prof. F. H. Schacher, Prof. U. S. Schubert
Laboratory of Organic and Macromolecular Chemistry (IOMC)
Friedrich Schiller University Jena
Humboldtstr. 10, 07743 Jena, Germany
E-mail: felix.schacher@uni-jena.de; ulrich.schubert@uni-jena.de
M. J. Barthel, T. Rudolph, A. Teichler, R. M. Paulus, Dr. J. Vitz, Dr. S. Hoeppener, Dr. M. D. Hager, Prof. F. H. Schacher, Prof. U. S. Schubert
Jena Center for Soft Matter (JCSM)
Friedrich-Schiller-University Jena
Philosophenweg 7, 07743 Jena, Germany
M. J. Barthel, A. Teichler, Dr. J. Vitz, Dr. S. Hoeppener, Prof. U. S. Schubert
Dutch Polymer Institute (DPI)
John F. Kennedylaan 2, 5612 AB Eindhoven, The Netherlands

DOI: 10.1002/adfm.201300469

The temperature-dependent reversible covalent crosslinking of polymers or block copolymers represents another interesting concept for the implementation of intrinsic self-healing into a material. Hereby, the Diels-Alder reaction represents a powerful tool.[21–27] One well-known example is the combination of furan and maleimide functionalities.[28–30] In this context, we have recently reported that furfuryl glycidyl ether can be used as a monomer for living anionic polymerization and the preparation of well-defined poly(ethylene oxide)-*b*-poly(furfuryl glycidyl ether) (PEO-*b*-PFGE) block copolymers comprising furan units in the side chain.[31] Subsequently, the furan units were used for the reversible core-crosslinking of the micelles formed by these block copolymers in selective solvents for the PEO segment. The application of polymer networks bearing free furan groups with a suitable linker (e.g., bismaleimides) in reversible Diels-Alder reactions represents a powerful system for potential self-healing applications.[21–24,28–30,32–34] This has been recently reported in the case of furfuryl glycidyl ether,[35,36] where the epoxy-ring was used in a condensation reaction with amino groups to create polymeric materials. These polymers can be turned into a network structure by reacting them with a bismaleimide compound.

We were now interested in exploiting the features of PEO-*b*-PFGE block copolymers for the generation of self-healing materials, in particular of nanostructured polymer films. Apart from the use of PEO-related materials in biological and medical context for PEG-ylation or drug-delivery approaches, PEO is widely used in the field of coatings. Here, antifouling properties, proliferated cell adhesion, or the coating of food supplement products have been described.[37–42] Moreover, the employment of block copolymers in self-healing applications represents an attractive approach. Such materials undergo microphase separation in bulk into a variety of well-documented morphologies.[43] In the case of AB diblock copolymers, this might be one way to solve a fundamental problem related to self-healing materials: the combination of strong reversible interactions between individual polymer chains together with dynamic properties (low glass transition temperature segments). However, such approaches have been rarely described,[44–48] as mostly statistical or random copolymers have been used for such purposes.

We herein describe the synthesis of well-defined PEO-*b*-PFGE block copolymers via living anionic ring-opening polymerization. Films of these materials were reversibly crosslinked using Diels-Alder (DA)/retro Diels-Alder (rDA) chemistry and investigated with regard to possible self-healing behavior. Multiple healing cycles as well as even complex damage patterns can be recovered, and the extent of the healing process (length, width of scratches as well as the time frame) were carefully investigated with a combination of differential scanning calorimetry (DSC), depth-sensing indentation, and profilometry studies. We further show that PEO-*b*-PFGE block copolymers undergo phase separation in the bulk, as indicated by small angle X-ray scattering, differential scanning calorimetry, and contact angle measurements.

2. Experimental Section

2.1. Instruments

^{1}H NMR spectra were recorded on a Bruker AC 300 MHz spectrometer in chloroform. Size exclusion chromatography (SEC) was performed on a Shimadzu SCL-10A system (with a LC-10AD pump, a RID-10A refractive index detector, and a PL gel 5 μm mixed-D column at RT), the eluent was a mixture of chloroform:triethylamine:*iso*-propanol (94:4:2) with a flow rate of 1 mL min^{-1}. The system was calibrated with poly(ethylene glycol) standards from PSS (M_n = 1470 g mol^{-1} to 42 000 g mol^{-1}). MALDI–ToF mass spectra were obtained using an Ultraflex III ToF/ToF mass spectrometer (Bruker Daltonics) with *trans*-2-[3-(4-*tert*-butylphenyl)-2-methyl-2-propenylidene] malononitrile (DCTB) or 2,5-dihydroxybenzoic acid (DHB) as matrix in reflector as well as in linear mode. The instrument was calibrated prior to each measurement with an external PMMA standard from PSS Polymer Standards Services GmbH. Surface topography as well as film thicknesses were measured using an optical interferometric profiler Wyko NT9100 (Veeco, Germany). The instrument is equipped with three objectives (2.5×, 5× and 20×), which enable effective magnifications between 1× to 40×. Differential scanning calorimetry (DSC) was performed on a Netzsch DSC 204 F1 equipped with a liquid nitrogen dewar. Dried samples were weighed into aluminum crucibles in amounts ranging from 5 to 20 mg, and an empty aluminum crucible was used as reference. The samples were measured with a temperature program consisting of three heating runs ranging from –150 to 150 °C with a heating rate of 20 K min^{-1} for the first heating run and 10 K min^{-1} for the second and third heating runs. The glass transition temperatures (T_g) were determined from the second and third heating runs (onset value). All thermograms were exported in graphs with exo down.

Mechanical Properties: The elastic moduli of the materials were characterized via depth-sensing indentation (DSI) using a TriboIndenter TI 900 (Hysitron Inc., Minneapolis, MN) with a NanoDMA 06 transducer, equipped with a conospherical diamond indenter tip of ≈4.7 μm radius. The polymer films were prepared by drop casting and dried afterwards under air. The measurements were conducted at ambient conditions, at 23 ± 1 °C and 31 ± 6% relative humidity (RH) for $PFGE_{55}$ and at 23 ± 1 °C and 30.0 ± 3% RH for PEO_{330}-*b*-$PFGE_{20}$, as measured with a Voltcraft DL–141TH data logger. For quasi-static testing, an open loop load function with 1 s loading, 2 s hold at maximum load, and 1 s unloading profile was applied.[49] All measurements were performed in a single automated run in less than 3 h for one sample. The reduced modulus E_r was determined from the unloading response using the analysis method proposed by Oliver and Pharr.[50] Measurements were repeated at sixteen maximum loads in a 4 × 4 array, for $PFGE_{55}$ increasing in steps of 120 μN from 100 to 1900 μN or in steps of 140 μN from 100 to 2200 μN, respectively. PEO_{330}-*b*-$PFGE_{20}$ was measured in steps of 100 μN from 100 to 1600 for the film and in steps of 120 μN from 100 to 1900 μN for the crosslinked sample. Values are averaged from at least ten measurements each. From the reduced modulus E_r, the indentation modulus

E_i was calculated using the elastic modulus and Poisson's ratio of the diamond indenter, 1140 GPa and 0.07, respectively, and a Poisson's ratio of 0.4 for the polymeric material, according to

$$E_{i,\text{sample}} = \frac{1 - v^2_{\text{sample}}}{\frac{1}{E_{r,\text{sample}}} - \frac{1-v^2_{\text{indenter}}}{E_{\text{indenter}}}} \quad (1)$$

The hardness is defined as:

$$H = \frac{P_{\max}}{A} \quad (2)$$

Small and Wide Angle X-Ray Scattering: SWAXS measurements on dried samples of $PFGE_{55}$ and PEO_{330}-*b*-$PFGE_{20}$ were performed on a Bruker AXS Nanostar (Bruker, Karlsruhe, Germany), equipped with a microfocus X-ray source (Incoatec IμSCu E025, Incoatec, Geesthacht, Germany), operating at λ = 1.54 Å. A pinhole setup with 750 μm, 400 μm, and 1000 μm (in the order from source to sample) was used and the sample-to-detector distance was 107 cm (SAXS) and 12 cm (WAXS). Samples were mounted on a metal rack and fixed using tape. The scattering patterns were corrected for the beam stop and the background (Scotch tape) prior to evaluations.

Transmission Electron Microscopy: performed using a TEM (Zeiss-CEM 902A, Oberkochen, Germany) operating at 80 kV. Images were recorded using a 1 k TVIPS FastScan CCD camera. The TEM samples were prepared by applying a drop of the sample solutions onto the surface of a carbon coated copper grid (Quantifoil Micro-Tools GmbH, Jena, Germany).

2.2. Materials

Ethylene oxide (EO) was purchased from Linde and Aldrich. Furfuryl glycidyl ether (FGE), *t*-BuOK, tetrahydrofuran (THF), *n*-hexane and toluene were purchased from Aldrich. Toluene and THF were used from a solvent purification system (PureSolv, Innovative Technology) and distilled over sodium/benzophenone. Ethylene oxide was distilled over sodium. Furfuryl glycidyl ether was purified by column chromatography (eluent: ethylacetate/*n*-hexane 5/1) and vacuum drying before usage. Diphenylmethyl potassium (DPMK) was synthesized as reported previously.[51] The PEO precursor was prepared via living anionic ring-opening polymerization of ethylene oxide with DPMK in THF in a BüchiGlasUster PicoClave and dried by azeotropic distillation under vacuum from dry toluene. *t*-BuOK was used as received.

Polymerization of FGE: 4 mL of freshly distilled THF were transferred into a Schlenk flask and 5.61 mg potassium *t*-butanolate (0.05 mmol) were added. Subsequently, 0.45 mL furfuryl glycidyl ether (FGE, 3.24 mmol, ratio of M:I was 65:1, $M_{n,\text{ theo}}$ = 10 000 g mol^{-1}) was introduced and the reaction was allowed to stir for 24 h at 45 °C. The reaction was terminated by adding 0.5 mL methanol and the product was washed with *n*-hexane and dried under vacuum.

^{1}H NMR (300 MHz, $CDCl_3$–d_6, δ): 7.27 (d, 1H, CH), 6.24–6.17 (m, 2H, CH), 4.35 (s, 2H, CH_2), 3.55–3.29 (br, 5H, backbone), 1.18 (s, 9H, *t*-Bu CH_3).

SEC: M_n = 2900 g mol^{-1}, M_w = 3100 g mol^{-1}, PDI = 1.07; MALDI–ToF MS: M_p = 8400 g mol^{-1}

Synthesis of PEO-b-PFGE Block Copolymers: PEO_{330}-*b*-$PFGE_{10}$: 3.45 g monohydroxy-functionalized PEO ($M_{n,\text{SEC}}$ = 14 000 g mol^{-1}, PDI = 1.05, $M_{p,\text{MALDI}}$ = 14 500 g mol^{-1}, 0.24 mmol) was dried under vacuum at 75 °C for 2 h and dissolved in 30 mL freshly distilled THF. To activate the hydroxyl group, a stoichiometric amount of DPMK was added until the solution remained slightly red. 0.33 mL (2.4 mmol) FGE was added and the reaction mixture was allowed to stir for 24 h at 45 °C under inert conditions. The reaction was terminated by the addition of 0.5 mL methanol and the crude polymer was purified by precipitation in cold diethyl ether and dried under vacuum.

^{1}H NMR (300 MHz, DMSO–d_6, δ): 7.5 (s, 1H, CH), 7.2–7.05 (m, 10H, Ar H), 6.3 (m, 2H, CH), 4.3 (s, 2H, CH_2), 3.95 (t, 1H, CH), 3.65–3.15 (br, PEO-backbone).

SEC: M_n = 15 200 g mol^{-1}, M_w = 16 100 g mol^{-1}, PDI = 1.06; MALDI–ToF MS: M_p = 16 000 g mol^{-1}

PEO_{330}-*b*-$PFGE_{20}$ was synthesized according the same procedure with regard to stoichiometry.

SEC: M_n = 17 600 g mol^{-1}, M_w = 18 100 g mol^{-1}, PDI = 1.04; MALDI–ToF MS: M_p = 17 000 g mol^{-1}

3. Results and Discussion

We have recently prepared well-defined PFGE homo- and PEO-*b*-PFGE block copolymers via living anionic ring-opening polymerization (AROP).[31] Herein, PEO-*b*-PFGE materials will be used for temperature-mediated self-healing of films after the controlled application of scratches. For this purpose two PEO-*b*-PFGE block copolymers, PEO_{330}-*b*-$PFGE_{10}$ and PEO_{330}-*b*-$PFGE_{20}$, were synthesized by sequential AROP and, for comparison, a $PFGE_{55}$ homopolymer (**Figure 1** and **Table 1**). Both PEO-*b*-PFGE block copolymers were prepared starting from a monohydroxy-PEO precursor by activation with diphenylmethyl potassium (DPMK), followed by the addition of FGE.[31]

3.1. Structural and Thermal Characterization of $PFGE_{55}$ and PEO_{330}-*b*-$PFGE_X$ Films

Both PFGE and PEO-*b*-PFGE block copolymers were investigated using differential scanning calorimetry (DSC, **Figure 2**).

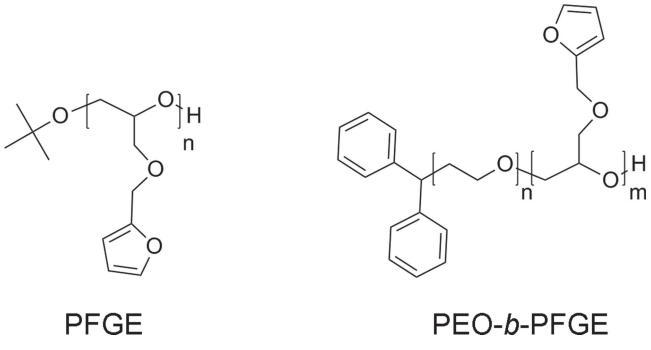

Figure 1. Schematic representation of the materials used in this study: PFGE and PEO-*b*-PFGE block copolymers.

Table 1. Characterization data of the used homo- and block copolymers.

Sample	$M_{n,theo}$ [g mol^{-1}]	$M_{n,SEC}$ [g mol^{-1}][b)]	$M_{p,MALDI}$ [g mol^{-1}]	PDI[b)]
$PFGE_{55}$	10 000	2900	8400	1.07
PEO_{330}[a)]	14 000	14 800	14 500	1.05
PEO_{330}-*b*-$PFGE_{10}$[c)]	16 000	15 200	16 000	1.06
PEO_{330}-*b*-$PFGE_{20}$[c)]	17 600	17 400	17 000	1.04

[a)]Precursor; [b)]Obtained by SEC ($CHCl_3$:TEA:i-Prop. 94:4:2, using PEO standards); [c)] Subscripts denote the degrees of polymerization of the corresponding block determined by ^{1}H NMR spectroscopy. The corresponding SEC traces, NMR spectra and MALDI-ToF MS pattern can be found in the Supporting Information, Figures S1–S3.

In addition, material degradation during the heating cycles, as well as the healing experiments discussed later, can be excluded, as thermogravimetric analysis (TGA) demonstrated thermal stability of the materials up to approximately 170 °C under air and 335 °C under nitrogen atmosphere (Supporting Information Figure S4).

As can be seen, the homopolymer $PFGE_{55}$ exhibits a T_g at approximately –40 °C (Figure 2a). PEO_{330}-*b*-$PFGE_{20}$ shows a strong melting peak at T_m = 59 °C, which can be attributed to the PEO segments (Figure 2b). The inset in Figure 2b shows the regime below 0 °C at higher resolution and reveals two separated glass transition temperatures at –79 and –40 °C, respectively. The first value can be assigned to PEO[52] whereas –40 °C reflects the PFGE segments. Both separate glass transition temperatures were also observed in case of PEO_{330}-*b*-$PFGE_{10}$ (data not shown here). The presence of two separated T_g's hints towards phase separation, although the overall molar mass of both PEO_{330}-*b*-$PFGE_X$ block copolymers is rather low. To confirm this assumption, additional SAXS experiments were performed on films which were annealed at 70 °C for 30 min and afterwards cooled to room temperature (Figure 2c).

Reflections could be observed for PEO_{330}-b-$PFGE_{20}$ at 0.46°, 0.92°, and 1.36°, corresponding to the [100]:[200]:[300] positions of a potential lamellar pattern, and the most intense [100] signal corresponds to a domain size of d_{lam} = 19 ± 2 nm. The formation of lamellae is rather surprising, as the volume fraction of PFGE in PEO_{330}-*b*-$PFGE_{20}$ is of about 17.5 wt%, rather hinting towards the formation of cylindrical domains. To probe the surface properties of the investigated films, water contact angle measurements were performed on PEO_{330}, $PFGE_{55}$, and PEO_{330}-*b*-$PFGE_{20}$ surfaces (Figure 2d). As expected, PEO_{330} shows a contact angle of 34.5°, which is characteristic for a hydrophilic surface, whereas this increases to 83.6° for $PFGE_{55}$. In case of PEO_{330}-*b*-$PFGE_{20}$, a value of 64.5° was obtained, showing surface characteristics in between the two corresponding homopolymers. At this point, we assume the

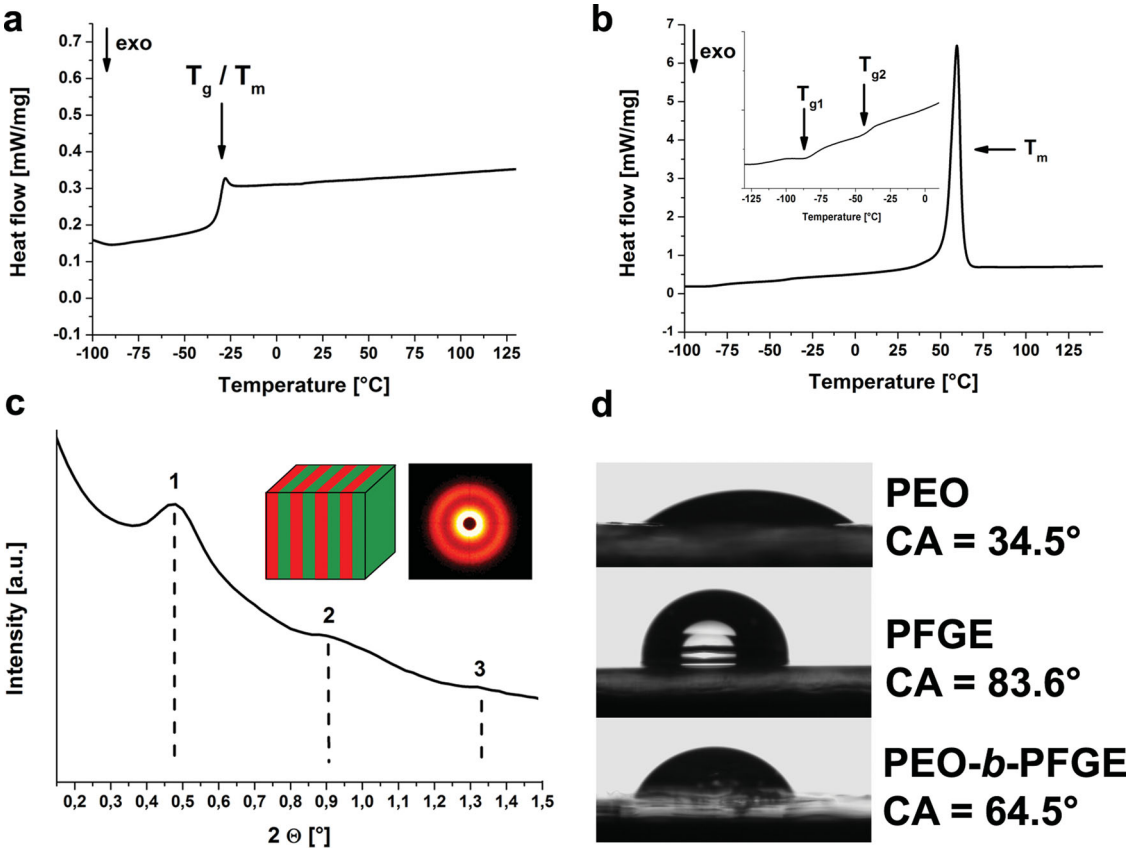

Figure 2. DSC thermograms of a) PFGE and b) PEO_{330}-*b*-$PFGE_{20}$. c) Zoom-in for PEO_{330}-*b*-$PFGE_{20}$. SAXS measurements of PEO_{330}-*b*-$PFGE_{20}$ and schematic representation of the proposed block copolymer bulk morphology. d) Contact angle measurements for PEO_{330}, $PFGE_{55}$ and PEO_{330}-*b*-$PFGE_{20}$.

formation of a lamellar bulk morphology in the case of PEO_{330}-*b*-$PFGE_{20}$. For PEO_{330}-*b*-$PFGE_{10}$, the obtained SAXS pattern (Supporting Information Figure S5a) was different, and the volume fraction of approximately 10% for PFGE hints towards the formation of PFGE spheres within a PEO matrix. This was confirmed by sonication-assisted dissolution of a crosslinked PEO_{330}-*b*-$PFGE_{10}$ block copolymer film in DMF, resulting in micellar structures with a crosslinked PFGE core of about 10 nm in diameter and a PEO corona, as observed via TEM measurements (Supporting Information, Figure S5b). Unfortunately, we were not able to distinguish between both domains in case of PEO_{330}-*b*-$PFGE_{20}$ block copolymers via atomic force microscopy (AFM) or TEM. In the latter case, thin samples (≈80 nm) were prepared from a crosslinked block copolymer film using a microtome. We observed rather rapid electron beam damage and the formation of sheet-like fragments. Even staining with OsO_4 (addressing any remaining double bonds in the PFGE domains) did not result in an improved phase contrast. As a consequence, the assumption of lamellar structures within films from PEO_{330}-*b*-$PFGE_{20}$ relies on the SAXS data, as well as contact angle measurements and the DSC results.

To exclude that the SAXS pattern in Figure 2c is merely caused by crystalline PEO domains, small (SAXS) and wide angle X-ray (WAXS) measurements at different temperatures were carried out (**Figure 3**). As it is clearly shown, the most intense reflection in SAXS at 0.46° is still present even above the melting point of PEO and after 16 h at 70 °C (Figure 3a). The fact that here only the [100] reflection is visible can be ascribed to shorter measurement times (≈30 min if compared to 4 h in Figure 2c), resulting in a decreasing signal-to-noise ratio. If this is combined with WAXS measurements of the same sample under comparable conditions (Figure 3b), very intense reflections at 18.6° and 22.8° (among other less intense signals) can be assigned to semicrystalline PEO domains.[53] Upon heating, these disappear at about 64 °C (inset in Figure 3b) and a broad amorphous halo can be observed.

3.2. Reversible Crosslinking of PFGE-Based Materials

For self-healing studies, films were prepared from $PFGE_{55}$, PEO_{330}-*b*-$PFGE_{10}$ and PEO_{330}-*b*-$PFGE_{20}$ via drop-casting onto polished glass slides. Typically, 20 mg of the polymer and a stoichiometric amount of the crosslinker, 1,1-diphenylmethyl bismaleimide (BMA), were dissolved in 0.2 mL dichloromethane (DCM). The solution was applied to a glass slide using a syringe and the solvent was allowed to evaporate.

Due to the presence of BMA, slightly yellow films (depending on the amount of crosslinker) were obtained. In case of the PFGE homopolymer, the amount of BMA was reduced to 0.8 equivalents, otherwise demixing and crystallization of the crosslinker was observed. For crosslinking, the polymer films were heated to 65 °C in an oven (**Figure 4**a). To ensure full crosslinking, the samples were kept at this temperature for 14 h. Subsequent network formation via crosslinking of the furan groups led to a significant change in the material properties, accompanied by a color change in case of the block copolymer films from slightly yellow to red. This was not the case for films from $PFGE_{55}$. We tentatively propose an aggregation of the crosslinker within the PEO domains, possibly due to the formation of π-complexes. This color change can also be monitored by time-dependent UV–Vis spectroscopy at 50 °C in solution (Supporting Information, Figure S6). However, the color change also depends on the temperature or the time during sample preparation. A detailed study of this phenomenon is, however, beyond the scope of this work. In all cases an increase of the film hardness was observed during crosslinking using depth sensing indentation measurements (Figure 4). We have to point out that films of PEO_{330}-*b*-$PFGE_{10}$ visibly melted at 59 °C even after crosslinking. As melting of crosslinked PEO_{330}-*b*-$PFGE_x$ films during the heating cycles would lead to film deformations, we focused on $PFGE_{55}$ and PEO_{330}-*b*-$PFGE_{20}$ for further studies.

First, the mechanical properties of PFGE-based films prior to and after crosslinking with BMA were investigated. As pristine films from $PFGE_{55}$ were liquid (highly viscous) at room-temperature, no indentation measurements were possible. PEO_{330}-*b*-$PFGE_{20}$ shows a hardness (*H*, defined as load/indentation area) of 0.038 GPa and a stiffness (E_i, Young modulus) of 0.46 GPa. All *H* values provided refer to a displacement of 150 nm. The E_i values represent average values of the obtained data in the linear range. After crosslinking, $PFGE_{55}$ shows a hardness of 0.6 GPa and a stiffness of E_i = 5.13 GPa (Figure 4b,d), the values being slightly higher as reported for "hard" polymers, like poly(methyl methacrylate) (PMMA, 0.32 GPa, 4.8 GPa) as well as polystyrene (PS, 0.34 GPa,

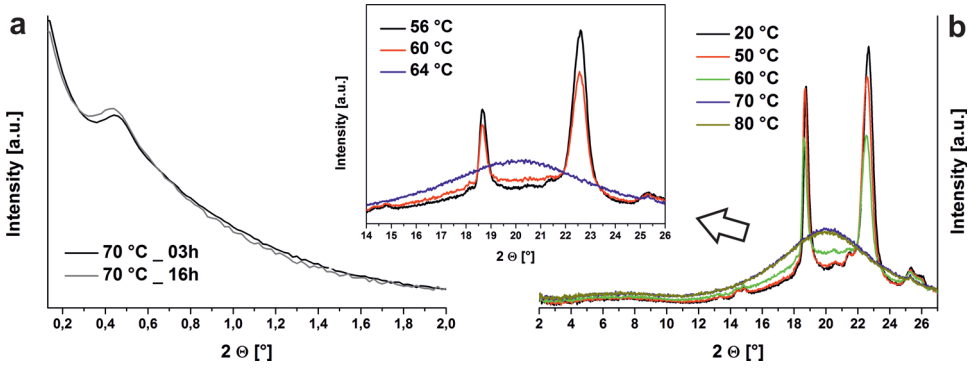

Figure 3. a) Small and b) wide angle X-ray patterns for PEO_{330}-*b*-$PFGE_{20}$ at different temperatures; the inset in (b) shows the enlarged region containing the reflexes for semicrystalline PEO.

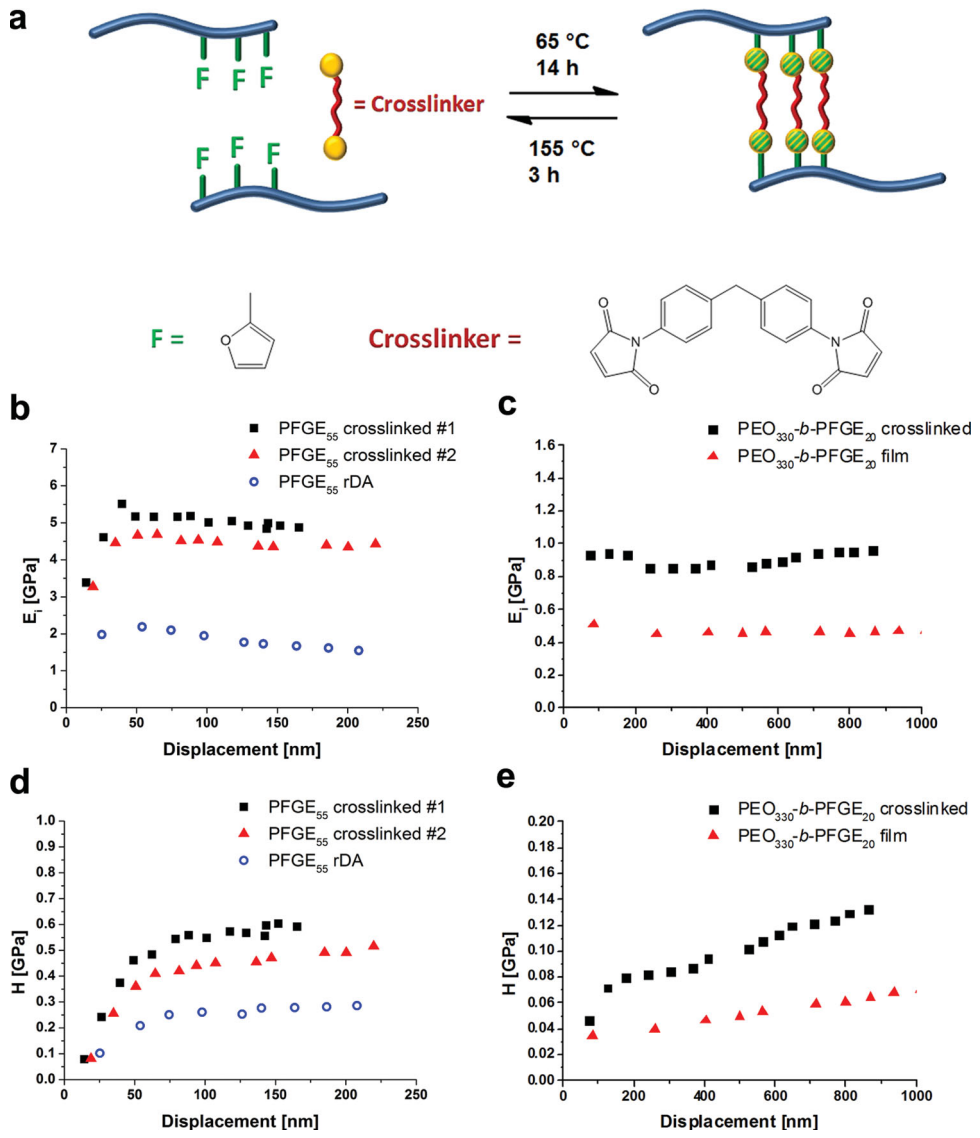

Figure 4. a) Schematic representation of the crosslinking of PFGE with a bifunctional maleimide BMA crosslinker. Depth-sensing indentation measurements for b,d) $PFGE_{55}$ and c,e) PEO_{330}-*b*-$PFGE_{20}$ films before and after crosslinking.

4.8 GPa).[54] This can be explained by a rather high degree of crosslinking, as each monomer unit carries a furan group in the side chain. For PEO_{330}-*b*-$PFGE_{20}$, significantly lower values of $H = 0.071$ GPa and $E_i = 0.91$ GPa compared to $PFGE_{55}$, but increased by a factor of two compared to the non-crosslinked state were obtained (Figure 4c,e). This can be rationalized by the presence of only 17 wt% PFGE and, hence, a lower overall degree of crosslinking.

According to the load displacement results, the block copolymer films showed visco-elastic behavior (Supporting Information, Figure S7), which is one prerequisite/driving force for a self-healing process. The PEO segments seemed to act as a softening material, whereas an increasing hardness at higher displacements was observed as well. The increase of both hardness and stiffness can be attributed to the crosslinking of $PFGE_{55}$ and PEO_{330}-*b*-$PFGE_{20}$ and, therefore, the rDA reaction is expected to invert this process. The films were therefore heated to 155 °C for 3 h and subjected to additional depth-sensing-indentation measurements at RT. At this point, a color change of the diblock copolymer film from red to brown was observed. Nevertheless, the block copolymer was shown to withstand these conditions.[31]

As expected, the E_i-modulus decreased to 1.76 GPa after the treatment at 155 °C, and the hardness was reduced to 0.26 GPa for $PFGE_{55}$ (Figure 4b,d). Subsequent re-crosslinking by heating to 65 °C for 14 h led to an increase to 4.51 GPa (E-modulus) and 0.45 GPa (hardness), although the values are slightly lower than after the first crosslinking procedure. We attribute this to an incomplete DA reaction. For the PEO_{330}-*b*-$PFGE_{20}$ block copolymer film, no significant changes after the rDA reaction were observed, which can be attributed to the rather low weight fraction of the PFGE segment.

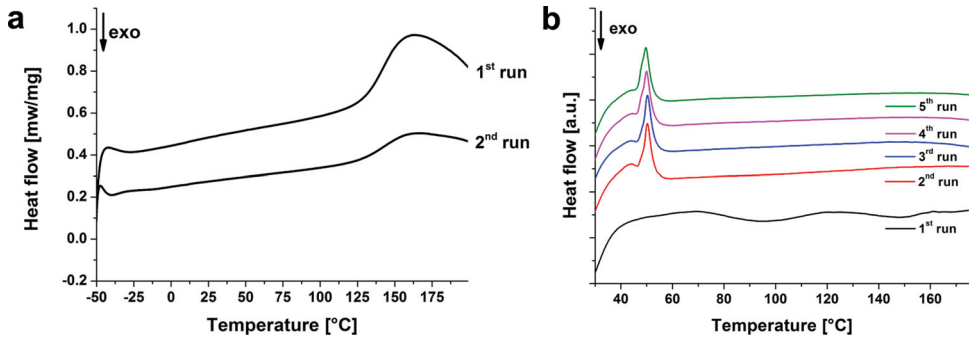

Figure 5. a) DSC measurements of a crosslinked $PFGE_{55}$ film with a heating rate of 20 K min^{-1} for the first run and 10 K min^{-1} for the second run. b) Multiple measurements of a crosslinked PEO_{330}-*b*-$PFGE_{20}$ block copolymer film.

As the rDA is the key for a successful reversible network formation, we studied a crosslinked $PFGE_{55}$ film in more detail by DSC measurements (**Figure 5**). As shown in Figure 5a for $PFGE_{55}$, the rDA reaction occurs within a temperature range of 135 to 160 °C. We attribute the fact that this is not visible for PEO_{330}-*b*-$PFGE_{20}$ to the limited sensitivity of the DSC and the low content of crosslinked furan rings. Heating of a crosslinked PEO_{330}-*b*-$PFGE_{20}$ does not reveal any signal during the first heating run (Figure 5b). However, after heating above the rDA temperature, subsequent cooling, and repeated heating a slight melting peak at 50 °C can be detected, which we ascribe to partial crystallization of the PEO domains.

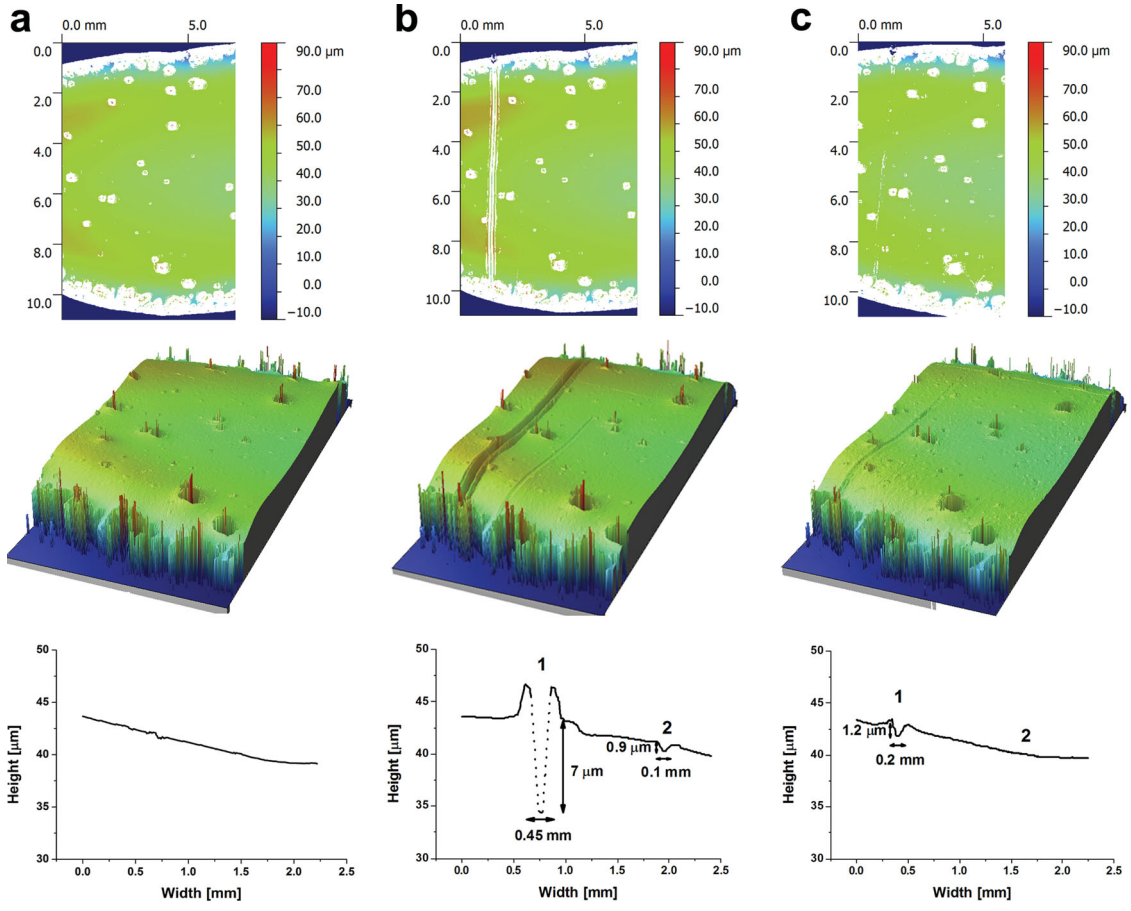

Figure 6. Profilometry measurements of PEO_{330}-*b*-$PFGE_{20}$ block copolymer films after a) crosslinking, b) scratching with a spatula, and c) the healing process at 155 °C.

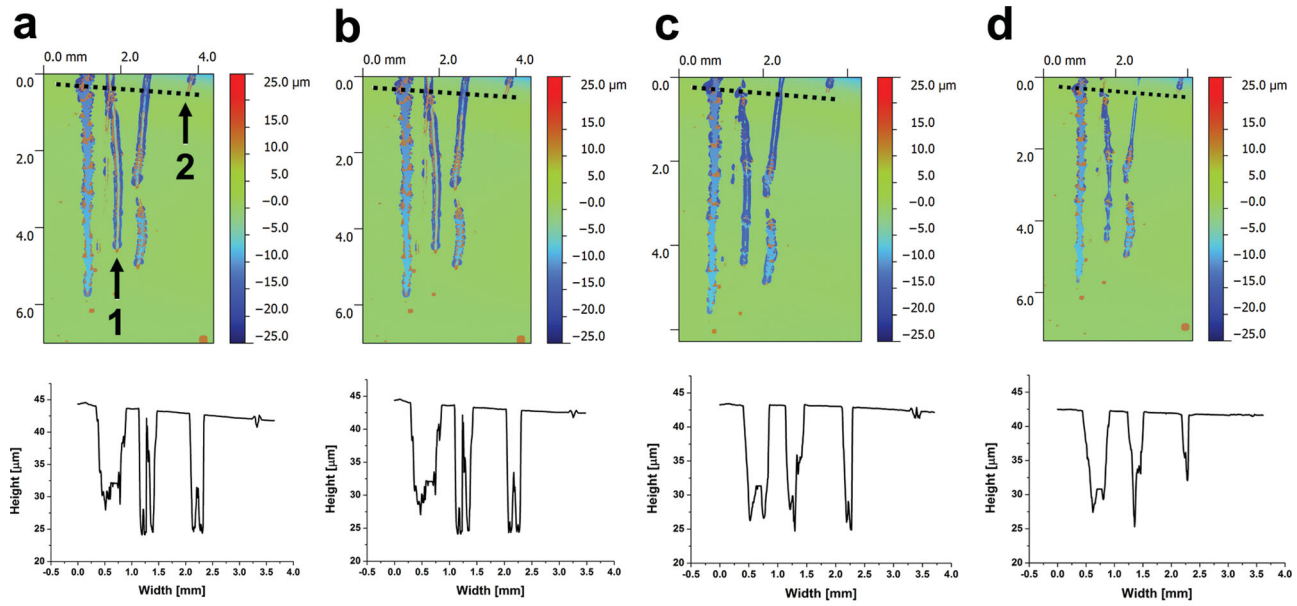

Figure 7. Profilometry measurements of a) a crosslinked PEO_{330}-*b*-$PFGE_{20}$ film, b) after heating for 4 h at 65 °C, c) subsequent heating for 4 h at 100 °C, and d) heating for 3 h at 155 °C.

3.3. Self-Healing Properties of PEO_{330}-*b*-$PFGE_{20}$

In order to introduce controlled surface defects, the respective films were treated with a spatula, resulting in scratches of varying depth, length and width. At this point, it can be noticed that such films from $PFGE_{55}$ were very brittle and scratching led to film breakage. Therefore, it was concluded that "pure" films from $PFGE_{55}$ are not suitable, at least as thin films, and we focused on PEO_{330}-*b*-$PFGE_{20}$ films, which were stable upon scratching.

Films containing PEO_{330}-*b*-$PFGE_{20}$ and the BMA crosslinker (molar ratio was 1:1) were prepared and crosslinked at 65 °C for 14 h. In the literature, values between 50 and 70 °C were determined for this procedure by DSC.[28,29,55,56] After crosslinking, the film surface was analyzed using an optical profilometer (**Figure 6**) and subsequently scratched with a spatula. As it can be seen, defined scratches (Scratch 1: 7 µm depth, 0.45 mm width, length 8 mm; Scratch 2: 0.9 µm depth, 0.1 mm width, length of 3.5 mm) were created (Figure 6b, the dashed lines are a guide to the eye as the instrument is not able to resolve the steep walls of this particular scratch). Afterwards, the block copolymer film was heated for 3 h at 155 °C, allowed to cool down slowly to 65 °C, and re-crosslinked for 14 h at 65 °C.

After the rDA reaction at 155 °C and subsequent crosslinking at 65 °C, profilometry revealed that Scratch 2 disappeared completely and Scratch 1 decreased to 1.2 µm depth and 0.2 mm width. Repetition of the heating process and increasing of the heating time did not lead to a further reduction of the scratch size. During all steps of this process, the overall thickness of the PEO_{330}-*b*-$PFGE_{20}$ film was monitored and shown to be constant (height ≈54 µm) (Supporting Information, Figure S8). Furthermore, defects within the block copolymer film remained unchanged, which would not be the case if the sample would undergo melting.

To ensure that the rDA reaction, followed by crosslinking at 65 °C, is responsible for the healing process, a film (**Figure 7**a) with defined scratches was heated for 4 h at 65 °C (over the melting temperature of the pristine block copolymer) and the surface was investigated by profilometry (Figure 7b). At this temperature, no changes were observed whereas subsequent heating to 100 °C for additional 4 h led to slight changes of the film surface (Figure 7c). In case of small scratches (max. depth 1 µm, Figure 7a,2), the depth was reduced by approximately 0.5 µm whereas deeper scratches (depth ≈6 µm or higher Figure 7a,1) remained unchanged. At this point we assume that heating to 100 °C leads to an increase of the chain mobility and possibly to the rDA reaction of small parts of the crosslinked units, which can be regarded as a kind of "pre-healing" process. Only if the film was heated to 155 °C for 3 h (Figure 7d), significant changes were observed (complete disappearance of smaller scratches as well as the decrease in length and width of larger defects). The fact that rather small gashes can already be repaired at lower temperatures has also been observed for networks from hyperbranched fluorinated polyethers created via DA chemistry.[57] Tentatively, the following mechanism is proposed to be responsible for the self-healing process: the incorporation of BMA and subsequent crosslinking leads to increasing hardness and decreasing chain mobility. At this point, the block copolymer film is damaged by mechanical force. Heating to 155 °C induces a rDA reaction and a partial decrosslinking of the network, accompanied by an increase in chain mobility leading to a kind of a reflow and, therefore, closure of the crack. The crosslinks are then partially reformed upon cooling.

We were also interested in the maximum number of possible self-healing cycles. For this purpose, a PEO_{330}-*b*-$PFGE_{20}$ block copolymer film was subjected to several cycles of crosslinking-scratching-rDA-crosslinking (**Figure 8**).

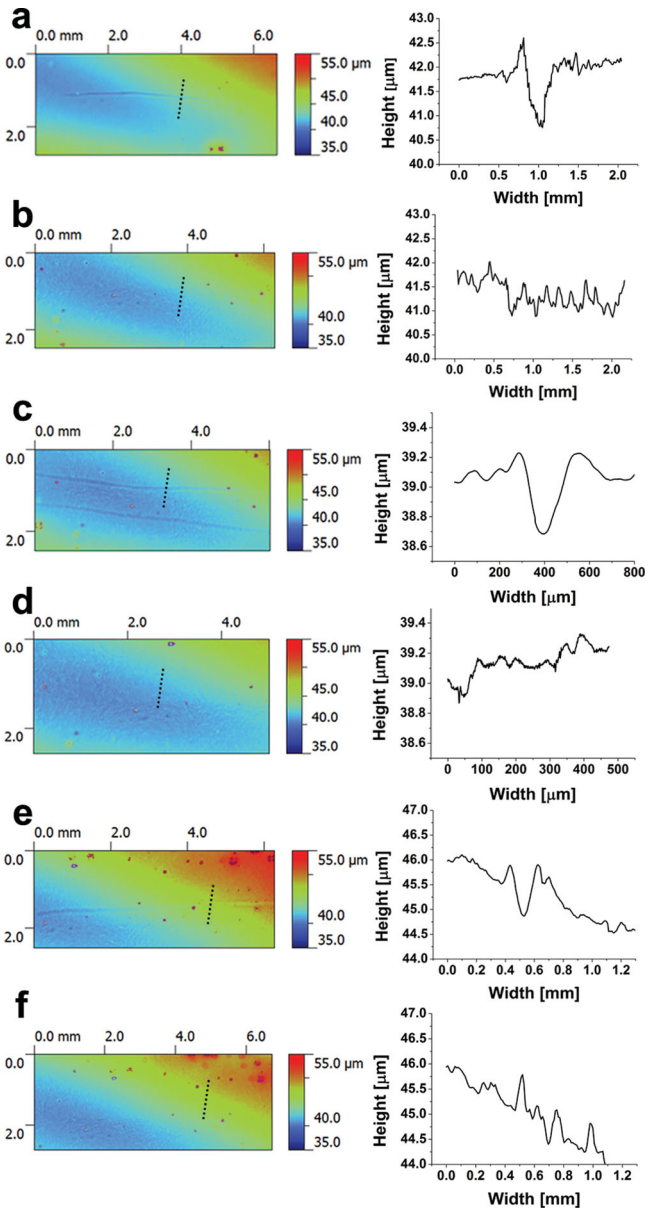

Figure 8. Repeated scratch healing of a PEO_{330}-*b*-$PFGE_{20}$ block copolymer film: 1st cycle a) after scratching; b) after healing, c,d) 2nd cycle, and e,f) 4th cycle.

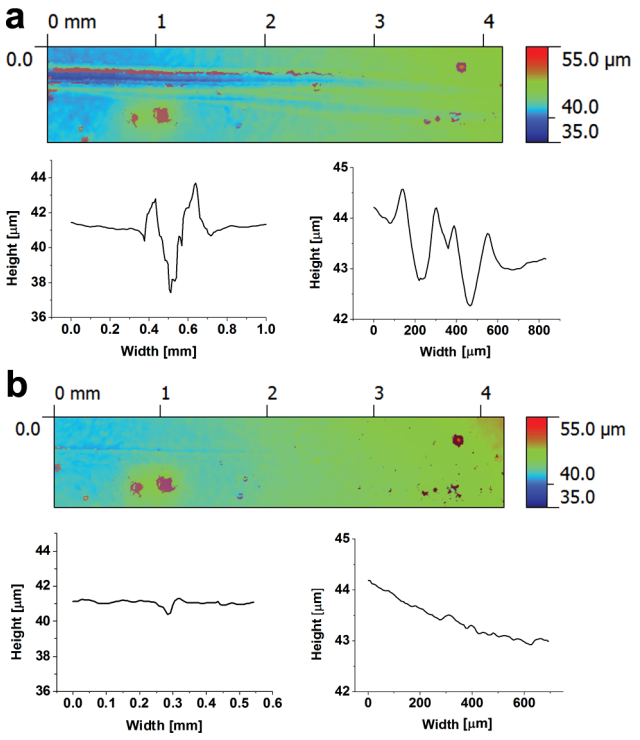

Figure 9. 5th scratch healing cycle of a PEO_{330}-*b*-$PFGE_{20}$ block copolymer film comprising a scratch with a gradient depth and width before (a) and after self-healing (b).

In the first cycle, a scratch of 0.13 mm width, 0.82 µm depth and 4.4 mm length was inflicted (Figure 8a), and heating to 155 °C for 3 h, followed by subsequent crosslinking for 14 h at 65 °C lead to a disappearance of the scratch (Figure 8b). This procedure was repeated 4 times, and the 2nd healing cycle (a scratch of 0.14 mm, 0.42 µm depth and 5.4 mm length) is shown in Figure 8c before and Figure 8d afterwards. Already here, it can be noticed that the film surface increases in roughness, particularly visible in the surface profile in Figure 8d. Nevertheless, in the fourth healing cycle, a 0.13 mm wide, 0.68 µm deep and 5.2 mm long scratch (Figure 8e) can be still removed (Figure 8f). Whereas this can be applied to rather small scratches, the efficiency of the healing process for the block copolymer films regarding larger surface defects seems to decrease with increasing cycle number. To demonstrate this, a scratch with a depth (3.8 to 1.3 µm) and width (3.4 to 1.7 mm) gradient was applied to a film after 4 healing cycles (**Figure 9**a). After heating to 155 °C for 3 h and subsequent crosslinking, the scratch depth decreased to 0.66 µm on the left side of the sample (Figure 9b). Also the width was reduced to 1.2 mm, whereas the thinner parts of the scratch completely disappeared. If compared to block copolymer films during the first healing cycles, where the depth of scratches could be reduced by up to 6–7 µm, this decreased after 5 healing cycles to approx. 2 to 3 µm.

Our explanation for this phenomenon is that with increasing number of heating cycles the amount of thermodynamically stable exo-product during the Diels-Alder reaction increases, which lead to a shift of the rDA process to higher temperatures.[58,59] As severe broadening of the signals in ^{1}H NMR spectroscopy hints towards (at least partial) material degradation when films were heated above 170 °C in air, a complete cleavage of the DA adducts is not possible under these conditions. As this currently limits the process, the films were heated under an inert atmosphere in a glovebox as an alternative. After 30 min at temperatures of 175 to 215 °C, a color change from brownish to dark brown was visible. Nevertheless, the network structure still seemed to be intact as the PEO_{330}-*b*-$PFGE_{20}$ film remained insoluble in different organic solvents (e.g., THF, DMF). To identify the origin of the color change, we heated pure PEO_{330}, $PFGE_{55}$ (pristine as well as crosslinked) and the BMA crosslinker was heated to 215 °C.

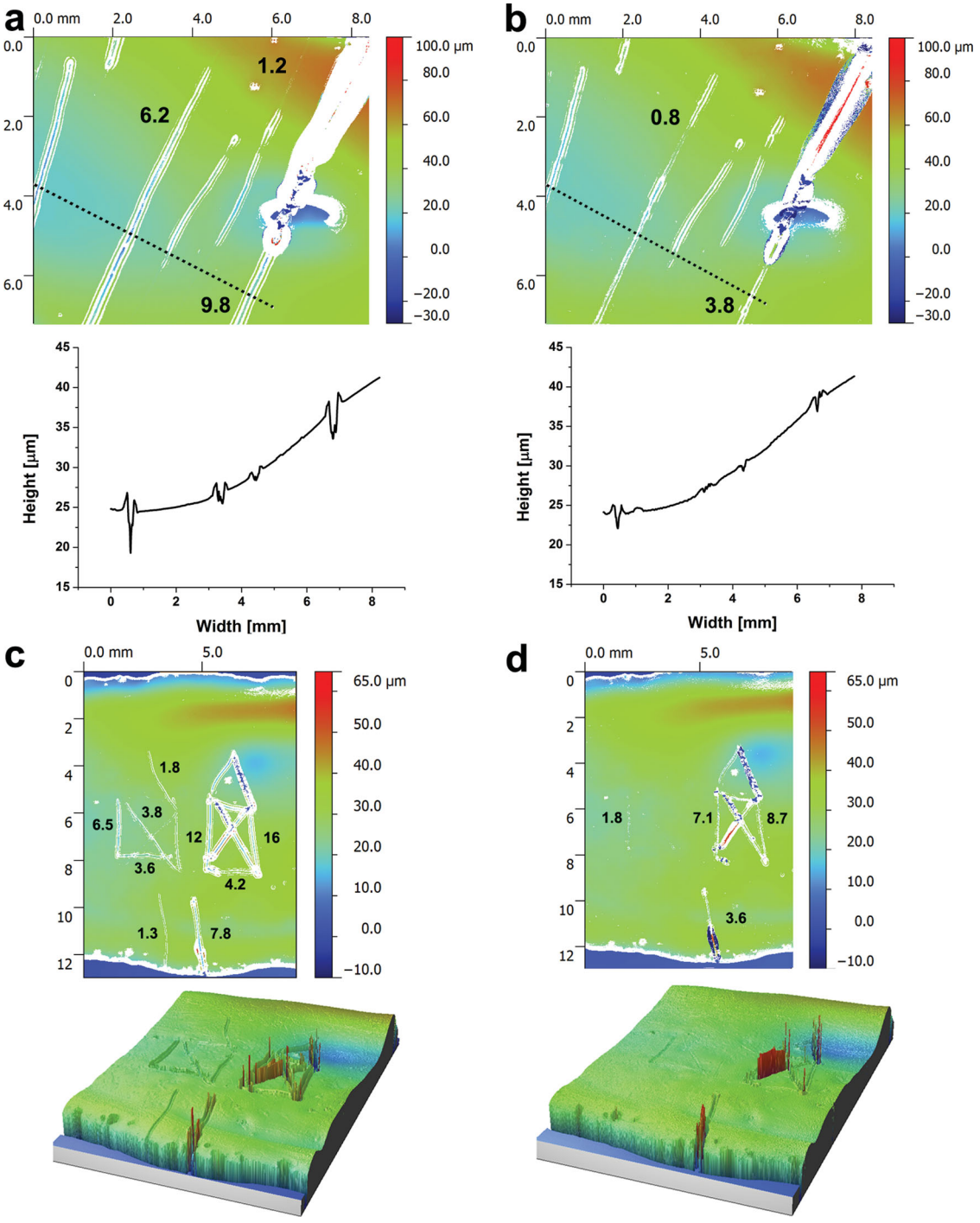

Figure 10. Self-healing process of a multi-scratch pattern (a) before, and b) after) as well as a complex pattern within a crosslinked PEO_{330}-*b*-$PFGE_{20}$ block copolymer film (c) before, and d) after heating to 155 °C).

Both PEO_{330} and BMA melted, whereas both PFGE samples revealed a rapid color change to dark brown, presumably due to the thermal instability of the furan moieties.[60] According to SEC measurements, no degradation occurred for $PFGE_{55}$ as a comparable elution trace was observed afterwards (Supporting Information, Figure S9). Nevertheless, we found that under these rather harsh conditions the surface roughness increased rapidly. This might be explained by a fast cooling of the sample and partial breakage of the film due to mechanical stress. Even after this heat treatment, the block copolymer films exhibited self-healing abilities (a scratch of 2.9 µm depth decreased to 0.3 µm).

3.4. Multiple Scratches and Complex Scratch Patterns

We also applied complex scratch patterns to crosslinked PEO_{330}-*b*-$PFGE_{20}$ block copolymer films (**Figure 10**). As shown in Figure 10b, small scratches with, e.g., a depth of 1.2 μm and a width of 0.16 mm disappeared completely, whereas deeper scratches with a depth of 6.2 or 9.8 μm and widths of 0.45 and 0.5 mm only decreased in size. The depths could be reduced to 0.8 and 3.8 μm, respectively, as well as the scratch width to 0.23 and 0.3 mm.

Figure 10c depicts a rather challenging scratch pattern, two "Santa's houses" with depths of approximately 1.8 to 6.8 μm and 4.2 to 16 μm. As shown in Figure 10d, the left (less deep) pattern vanished nearly completely. Only in case of the deeper scratch (6.5 μm), the depth was reduced to 1.8 μm, whereas the right-hand pattern comprising deeper scratches (12 to 16 μm) can still be seen afterwards (remaining scratches with 7.1 and 8.7 μm depth).

Finally, the comparison of the healing efficiency of the system presented here with literature examples was targeted. As shown before, it is possible to heal scratches of up to 6 μm depth and 1.7 mm width at elevated temperatures and on a time scale of 17 h (3 h at 155 °C and 14 h at 65 °C). One of the next targets for future studies is to reduce the required annealing times. For the initial investigation of the system the focus was placed on the complete crosslinking of the polymer films. However, self-healing approaches exploiting Diels-Alder chemistry will be necessarily limited to this temperature range in order to induce network formation or cleavage. This has also been demonstrated for comparable systems using this approach.[29,35] Self-healing processes based on π–π interactions have been shown to operate at 90 °C and were able to cure scratches of up to 75 μm width within minutes.[20] In the case of systems based on hydrogen bonding it could be shown that previously cut pieces reconnect by simple surface contact at ambient temperatures, but this ability decreased the longer the pieces were kept separate (which we did not observed in the current example).[15,61] Comparable materials based on reversible metal-ligand-interactions were also healed at elevated temperatures (>100 °C) and the BMA crosslinker to 215 °C.[17,18,62]

4. Conclusion

We demonstrate one of the first examples for self-healing materials based on block copolymers. Films from PEO_{330}-*b*-$PFGE_{20}$ diblock copolymers were shown to exhibit a smooth surface and a lamellar bulk morphology with a domain size of approximately 19 nm. The materials are capable of undergoing reversible (up to five times shown here) crosslinking/de-crosslinking and, hence, healing of inflicted damage at elevated temperatures. Comparison with $PFGE_{55}$ homopolymers via depth-sensing indentation revealed that this is accompanied by changes in hardness of the PFGE minority fraction. The results clearly show that PEO-*b*-PFGE block copolymers are promising candidates for self-healing surfaces (possible healing of scratches of up to 6 μm depth and 1.7 mm width), although still rather long cycles (up to 17 h) and high temperatures (155 °C) are required, and the employed BMA crosslinker is rather toxic. In addition, the efficiency of the rDA process decreases with increasing cycle number, presumably due to the formation of the exo-product during the DA reaction. Nevertheless, our approach addresses one of the inherent problems in self-healing materials: the combination of smooth and dynamic segments with the capability of strong and reversible network formation via, here, Diels-Alder chemistry.

It will be the subject of further studies to purposefully vary the weight fraction of PFGE to access different bulk morphologies for such block copolymers as well as to identify superior crosslinking agents. Also, the use of PFGE-*b*-PEO-*b*-PFGE triblock copolymers might be advantageous.

Supporting Information

Supporting Information is available from the Wiley Online Library or from the author.

Acknowledgements

The authors thank Steffi Stumpf for help with AFM measurements, Sarah Crotty for MALDI-ToF-MS measurements and Ulrike Günther for help with the sample preparation for TEM measurements. We also wish to acknowledge the Dutch Polymer Institute (DPI, technology area high-throughput-experimentation, project #690) and the Thuringian Ministry for Education, Science and Culture (grants #B514-09051, NanoConSens and #B515-11028, SWAXS-JCSM) for financial support of this study. F. H. S. and T. R. are further grateful to the Thuringian Ministry for Education, Science, and Culture (TMBWK; #B515-10065, ChaPoNano). T. R. acknowledges the Carl-Zeiss foundation for a PhD-scholarship. U. S. S. and M. D. H. thank the DFG for financial support within the framework of SPP 1568.

Received: February 4, 2013
Revised: February 26, 2013
Published online: April 19, 2013

[1] M. D. Hager, P. Greil, C. Leyens, S. van der Zwaag, U. S. Schubert, *Adv. Mater.* **2010**, *22*, 5424–5430.
[2] R. S. Trask, H. RWilliams, I. P. Bond, *Bioinspir. Biomim.* **2007**, *2*, P1–P9.
[3] E. W. Davie, O. D. Ratnoff, *Science* **1964**, *145*, 1310-&.
[4] E. Vaccaro, J. H. Waite, *Biomacromolecules* **2001**, *2*, 906–911.
[5] B. J. Blaiszik, S. L. B. Kramer, S. C. Olugebefola, J. S. Moore, N. R. Sottos, S. R. White, *Annu. Rev. Mater. Res.* **2010**, *40*, 179–211.
[6] N. K. Guimard, K. K. Oehlenschlaeger, J. W. Zhou, S. Hilf, F. G. Schmidt, C. Barner-Kowollik, *Macromol. Chem. Phys.* **2012**, *213*, 131–143.
[7] S. Bode, B. Sandmann, M. D. Hager, U. S. Schubert, *Metal-Complex based Self-healing Polymers* in *Self-Healing Polymers: From Principles to Applications* (Ed. W. Binder), Wiley-VCH, Weinheim **2013**.
[8] S. R. White, N. R. Sottos, P. H. Geubelle, J. S. Moore, M. R. Kessler, S. R. Sriram, E. N. Brown, S. Viswanathan, *Nature* **2001**, *409*, 794–797.
[9] H. R. Williams, R. S. Trask, P. M. Weaver, I. P. Bond, *J. R. Soc. Interface* **2008**, *5*, 55–65.
[10] V. Berl, M. Schmutz, M. J. Krische, R. G. Khoury, J. M. Lehn, *Chem-Eur. J.* **2002**, *8*, 1227–1244.
[11] J. L. Wietor, A. Dimopoulos, L. E. Govaert, R. A. T. M. van Benthem, G. de With, R. P. Sijbesma, *Macromolecules* **2009**, *42*, 6640–6646.

[12] R. P. Sijbesma, F. H. Beijer, L. Brunsveld, B. J. B. Folmer, J. H. K. K. Hirschberg, R. F. M. Lange, J. K. L. Lowe, E. W. Meijer, *Science* **1997**, *278*, 1601–1604.
[13] O. A. Scherman, G. B. W. L. Ligthart, R. P. Sijbesma, E. W. Meijer, *Angew. Chem. Int. Ed.* **2006**, *45*, 2072–2076.
[14] H. Ohkawa, G. B. W. L. Ligthart, R. P. Sijbesma, E. W. Meijer, *Macromolecules* **2007**, *40*, 1453–1459.
[15] P. Cordier, F. Tournilhac, C. Soulie-Ziakovic, L. Leibler, *Nature* **2008**, *451*, 977–980.
[16] D. Montarnal, M. Capelot, F. Tournilhac, L. Leibler, *Science* **2011**, *334*, 965–968.
[17] S. Bode, L. Zedler, F. H. Schacher, B. Dietzek, M. Schmitt, J. Popp, M. D. Hager, U. S. Schubert, *Adv. Mater.* **2013**, *25*, 1634–1638.
[18] M. Burnworth, L. M. Tang, J. R. Kumpfer, A. J. Duncan, F. L. Beyer, G. L. Fiore, S. J. Rowan, C. Weder, *Nature* **2011**, *472*, 334–337.
[19] S. Burattini, B. W. Greenland, W. Hayes, M. E. Mackay, S. J. Rowan, H. M. Colquhoun, *Chem. Mater.* **2011**, *23*, 6–8.
[20] S. Burattini, H. M. Colquhoun, J. D. Fox, D. Friedmann, B. W. Greenland, P. J. F. Harris, W. Hayes, M. E. Mackay, S. J. Rowan, *Chem. Commun.* **2009**, 6717–6719.
[21] X. X. Chen, M. A. Dam, K. Ono, A. Mal, H. B. Shen, S. R. Nutt, K. Sheran, F. Wudl, *Science* **2002**, *295*, 1698–1702.
[22] X. X. Chen, F. Wudl, A. K. Mal, H. B. Shen, S. R. Nutt, *Macromolecules* **2003**, *36*, 1802–1807.
[23] Y. L. Liu, C. Y. Hsieh, *J. Polym. Sci. Part A: Polym. Chem.* **2006**, *44*, 905–913.
[24] M. Wouters, E. Craenmehr, K. Tempelaars, H. Fischer, N. Stroeks, J. van Zanten, *Prog. Org. Coat.* **2009**, *64*, 156–162.
[25] J. Zhou, N. K. Guimard, A. J. Inglis, M. Namazian, C. Y. Lin, M. L. Coote, E. Spyrou, S. Hilf, F. G. Schmidt, C. Barner-Kowollik, *Polym. Chem.* **2012**, *3*, 628–639.
[26] A. J. Inglis, L. Nebhani, O. Altintas, F. G. Schmidt, C. Barner-Kowollik, *Macromolecules* **2010**, *43*, 5515–5520.
[27] J. Kötteritzsch, S. Stumpf, S. Hoeppener, J. Vitz, M. D. Hager, U. S. Schubert, *Macromol. Chem. Phys.* **2013**, DOI: 10.1002/macp.201200712.
[28] A. Gandini, *Prog. Polym. Sci.* **2013**, *38*, 1–29.
[29] Y. Zhang, A. A. Broekhuis, F. Picchioni, *Macromolecules* **2009**, *42*, 1906–1912.
[30] J. A. Syrett, C. R. Becer, D. M. Haddleton, *Polym. Chem.* **2010**, *1*, 978–987.
[31] M. J. Barthel, T. Rudolph, S. Crotty, F. H. Schacher, U. S. Schubert, *J. Polym. Sci. Part A: Polym. Chem.* **2012**, *50*, 4958–4965.
[32] R. Gheneim, C. Perez-Berumen, A. Gandini, *Macromolecules* **2002**, *35*, 7246–7253.
[33] Q. Tian, Y. C. Yuan, M. Z. Rong, M. Q. Zhang, *J. Mater. Chem.* **2009**, *19*, 1289–1296.
[34] C. Gousse, A. Gandini, P. Hodge, *Macromolecules* **1998**, *31*, 314–321.
[35] P. A. Pratama, A. M. Peterson, G. R. Palmese, *Macromol. Chem. Phys.* **2012**, *213*, 173–181.
[36] A. M. Peterson, R. E. Jensen, G. R. Palmese, *ACS Appl. Mater. Interfaces* **2010**, *2*, 1141–1149.
[37] T. Ekblad, G. Bergstroem, T. Ederth, S. L. Conlan, R. Mutton, A. S. Clare, S. Wang, Y. L. Liu, Q. Zhao, F. D'Souza, G. T. Donnelly, P. R. Willemsen, M. E. Pettitt, M. E. Callow, J. A. Callow, B. Liedberg, *Biomacromolecules* **2008**, *9*, 2775–2783.
[38] H. Xu, F. Yan, E. E. Monson, R. Kopelman, *J. Biomed. Mater. Res. A* **2003**, *66A*, 870–879.
[39] *EFSA J.* **2006**, *4*, 414–415.
[40] I. Banerjee, R. C. Pangule, R. S. Kane, *Adv. Mater.* **2011**, *23*, 690–718.
[41] P. Kim, D. H. Kim, B. Kim, S. K. Choi, S. H. Lee, A. Khademhosseini, R. Langer, K. Y. Suh, *Nanotechnology* **2005**, *16*, 2420–2426.
[42] N. A. Peppas, J. Z. Hilt, A. Khademhosseini, R. Langer, *Adv. Mater.* **2006**, *18*, 1345–1360.
[43] F. H. Schacher, P. A. Rupar, I. Manners, *Angew. Chem. Int. Ed.* **2012**, *51*, 7898–7921.
[44] P. Tyagi, A. Deratani, D. Bouyer, D. Cot, V. Gence, M. Barboiu, T. N. T. Phan, D. Bertin, D. Gigmes, D. Quemener, *Angew. Chem. Int. Ed.* **2012**, *51*, 7166–7170.
[45] K. J. Henderson, T. C. Zhou, K. J. Otim, K. R. Shull, *Macromolecules* **2010**, *43*, 6193–6201.
[46] M. D. Chipara, M. Chipara, E. Shansky, J. M. Zaleski, *Polym. Adv. Technol.* **2009**, *20*, 427–431.
[47] J. Hentschel, A. M. Kushner, J. Ziller, Z. Guan, *Angew. Chem.* **2012**, *51*, 10561.
[48] A. A. Kavitha, N. K. Singha, *Macromolecules* **2010**, *43*, 3193–3205.
[49] E. F. J. Rettler, J. M. Kranenburg, H. M. L. Lambermont-Thijs, R. Hoogenboom, U. S. Schubert, *Macromol. Chem. Phys.* **2010**, *211*, 2443–2448.
[50] W. C. Oliver, G. M. Pharr, *J. Mater. Res.* **1992**, *7*, 1564–1583.
[51] H. Normant, B. Angelo, *B. Soc. Chim. Fr.* **1960**, 354–359.
[52] E. Araneda, A. Leiva, L. Gargallo, N. Hadjichristidis, I. Mondragon, D. Radic, *Polym. Eng. Sci.* **2012**, *52*, 1128–1136.
[53] F. H. Schacher, J. Elbert, S. K. Patra, S. F. M. Yusoff, M. A. Winnik, I. Manners, *Chem-Eur. J.* **2012**, *18*, 517–525.
[54] B. J. Briscoe, L. Fiori, E. Pelillo, *J. Phys. D. Appl. Phys.* **1998**, *31*, 2395–2405.
[55] J. A. Syrett, G. Mantovani, W. R. S. Barton, D. Price, D. M. Haddleton, *Polym. Chem.* **2010**, *1*, 102–106.
[56] C. Toncelli, D. C. De Reus, F. Picchioni, A. A. Broekhuis, *Macromol. Chem. Phys.* **2012**, *213*, 157–165.
[57] P. M. Imbesi, C. Fidge, J. E. Raymond, S. I. Cauët, K. L. Wooley, *ACS Macro Lett.* **2012**, *1*, 473–477.
[58] J. Canadell, H. Fischer, G. De With, R. A. T. M. Van Benthem, *J. Polym. Sci. Part A: Polym. Chem.* **2010**, *48*, 3456–3467.
[59] L. Rulisek, P. Sebek, Z. Havlas, R. Hrabal, P. Capek, A. Svatos, *J. Org. Chem.* **2005**, *70*, 6295–6302.
[60] S. D. Bergman, F. Wudl, *J. Mater. Chem.* **2008**, *18*, 41–62.
[61] G. M. L. van Gemert, J. W. Peeters, S. H. M. Sontjens, H. M. Janssen, A. W. Bosman, *Macromol. Chem. Phys.* **2012**, *213*, 234–242.
[62] J. Yuan, X. Fang, L. Zhang, G. Hong, Y. Lin, Q. Zheng, Y. Xu, Y. Ruan, W. Weng, H. Xia, G. Chen, *J. Mater. Chem.* **2012**, *22*, 11515–11522.